Engh et al, http://www.jgp.org/cgi/doi/10.1085/jgp.200709760

Our computational analysis relies on the assumption that our homology model represents the structure of ClC-0 approximately, particularly in the vicinity of the binding sites. Although in the absence of other structures it is difficult to test this assumption, we can test to see if small variations around that structural model, e.g., 0.3–0.5 Å, affect the results critically. Since in reality such variations may arise simply from the thermal fluctuations of the protein structure, it is legitimate to ask if using a single static structure is appropriate, and worthwhile to determine the sensitivity of our calculations to the exact set of structural coordinates used.

To address this question, we generated two ensembles of 100 conformations each, one for WT and one for K149L, and performed the same Poisson-Boltzmann calculations for each conformation as for the original models. Each ensemble of conformations was generated by running short (10 ps) Langevin dynamic simulations of the homology model with most of the structure fixed in space. However, the residues in the vicinity of the chloride binding sites were not fixed; these are 122–126 (loop CD), 149, 416–418, and 512. A soft restraining (harmonic) potential with the strength tuned accordingly was used to sample conformations in the 0.3–0.5 Å range (final force constant 0.25 $k_BT/$ Å^2). No solvent or membrane was included, but a distance-dependent dielectric constant was used to approximate the electrostatics in the pore. Physiological temperature was used (300°K) and the friction constant was 5 ps^{-1}.

Fig. S6 A shows a molecular graphics overlay of the 100 conformations derived for the wild-type homology model (left) and the K149L homology model (right), with the chloride ions in their fixed positions, as in the original homology model. For the residues that were allowed to move, we calculated the pairwise root-mean-square deviation (pairwise RMSD) for every pair of conformations in the ensemble. Fig. S6 B shows the distribution of those values. These distributions illustrate that the simulation conditions we used did in fact result in structural variations in the 0.3–0.5 Å range, and that there is no major difference between the distribution of wild type and K149L

To derive the characteristic electrostatic binding energies for each of the ensembles, we performed a Poisson-Boltzmann calculation for each conformation. Fig. S6 C shows that in no case is the electrostatic binding energy for an ensemble significantly different from that

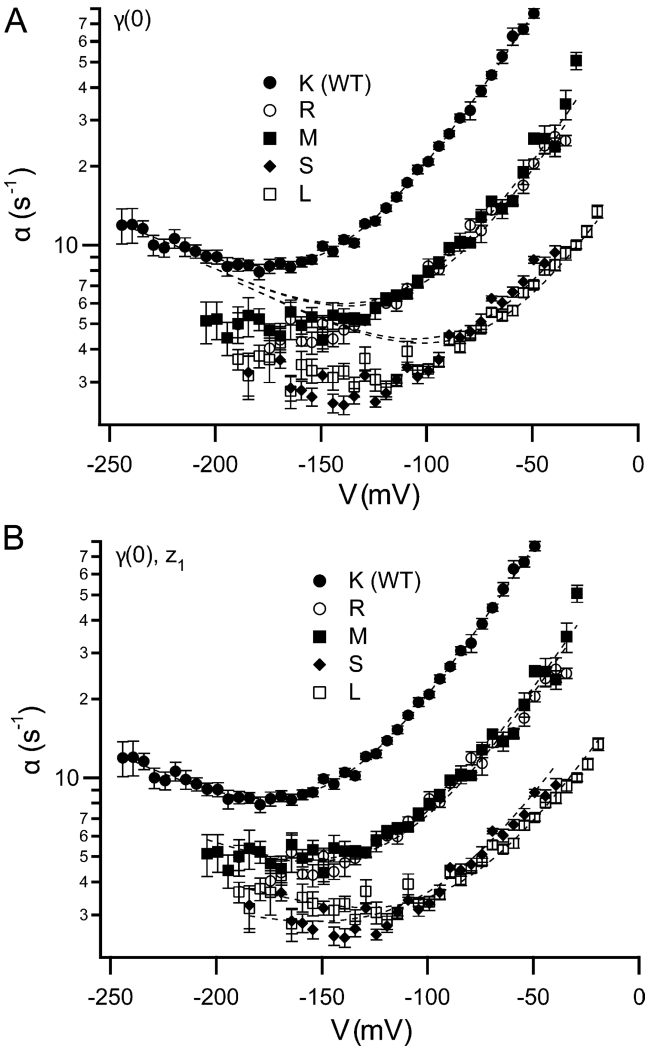

Figure S1. Effects of K149 mutations on the opening rate constant: initial fits to the five-state model. This figure is analogous to Fig. 4 in the manuscript. The voltage dependence of the opening rate constant (α) for wild type and for selected K149 mutants at 110 mM external chloride was fit to the five-state model shown in Scheme II. Fits are shown as dashed lines. Wild-type data were fit by letting all six parameters in the model vary. For mutant data, fits were derived by letting vary only γ(0) (A), or only γ(0) and z_1 (B), while holding all other parameters at their wild-type best-fit values. The fits in B yielded γ(0) values for wild type, K149R, M, S, L, in s^{-1}: 464, 122, 128, 45, 33; and corresponding z_1 values: −0.24, −0.19, −0.19, −0.11, −0.15. For each voltage, the opening rate constant (α) was derived using data from at least five patches. These opening rate constants were averaged and the error bars show the SEM.

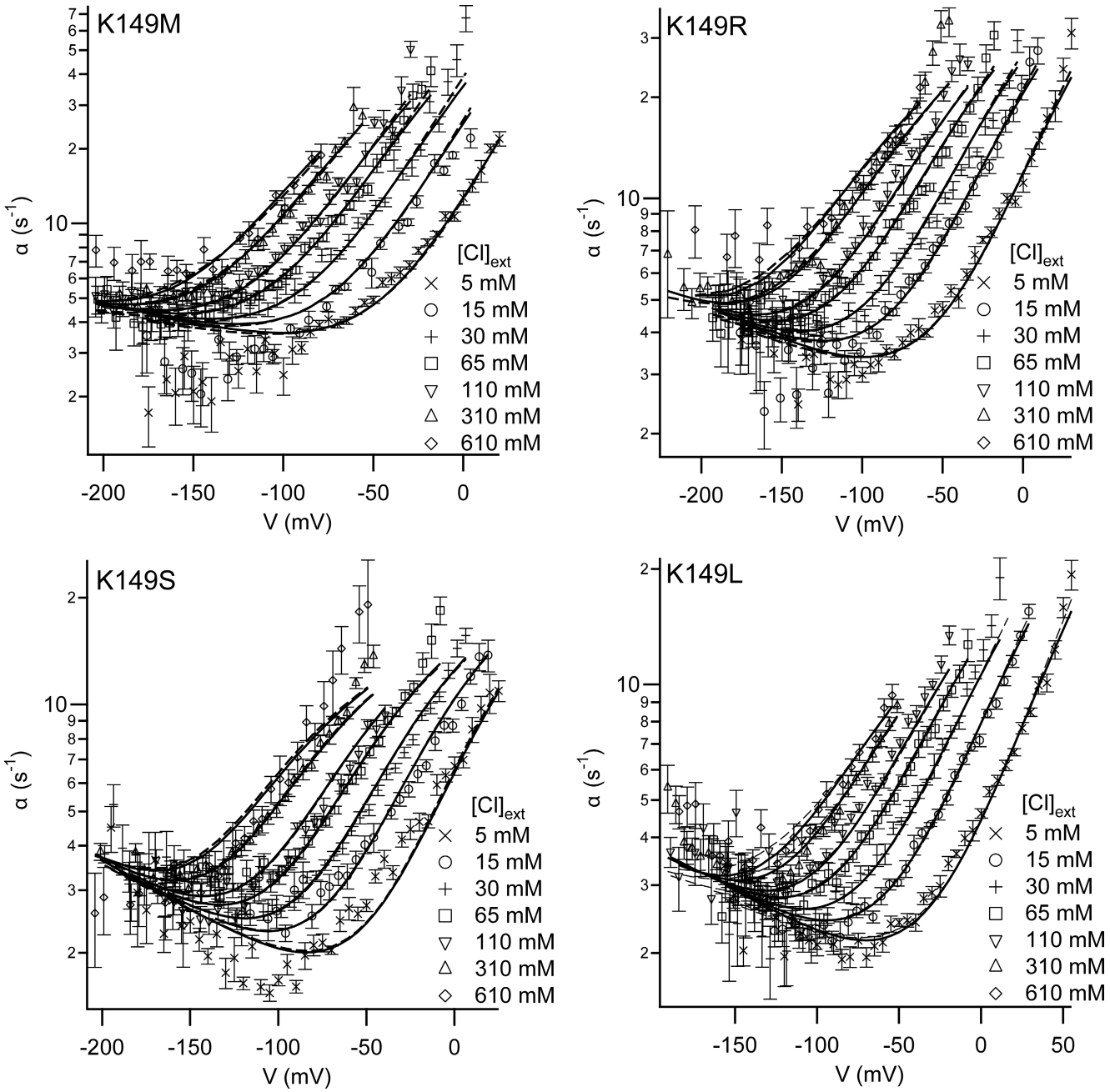

Figure S2. Effects of K149 mutations on the opening rate constant: external chloride dependence and fits to the gating models. This figure is analogous to Fig. 6 in the manuscript. The opening rate constant (α) as a function of voltage (V) and external chloride ($[Cl]_{ext}$) is shown for mutants K149 M, R, S, and L. Each dataset was globally fit to the four-state (Scheme I) and five-state (Scheme II) models proposed by Chen and Miller (1996) (dashed lines and solid lines, respectively). The resulting parameter values are shown in Figs. 7 and S3. For each condition (V, $[Cl]_{ext}$), the opening rate constant (α) was derived using data from at least five patches. These opening rate constants were averaged and the error bars show the SEM.

of its corresponding single model. Thus the calculations of the electrostatic contribution to chloride binding given in the original manuscript, which are each based on a single static structure, are representative of the corresponding ensemble calculations.

In conclusion, the effect of the K149 mutation on the electrostatic contribution to chloride binding affinity is similar whether the single model or an ensemble of conformations (within 0.5 Å) is used in the calculations.

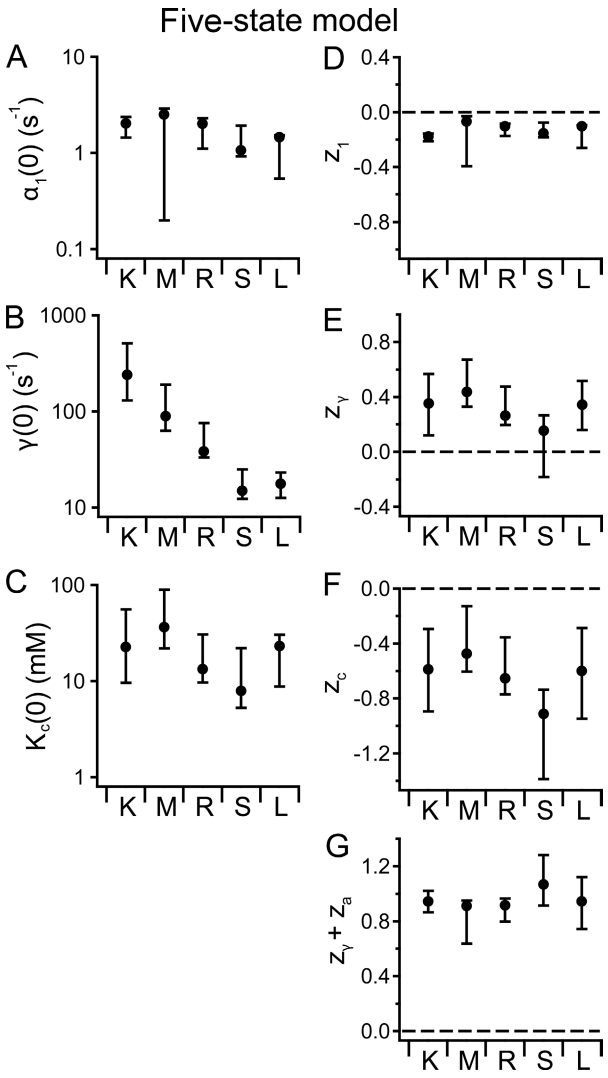

Figure S3. Best-fit values for the five-state model gating parameters. (A–F) The opening rate constant as a function of voltage and chloride ($\alpha(V, [Cl]_{ext})$) was globally fit to the five-state model (see Fig. S2), and the best fit values for the six parameters in the model are plotted for wild-type (K) and the four K149 mutants (M, R, S, L). $K_c(0)$ is given in terms of chloride activity. (G) The total charge that moves during depolarization-activated gating (the K_c step followed by the γ step) was calculated by adding z_γ (the charge that moves during the γ step) to z_a (the charge that moves during the K_c step, which is equal to $-z_c$). Error bars show the 95% confidence limits determined as described in Engh, A.M., J.D. Faraldo-Gómez, and M. Maduke. 2007. *J. Gen. Physiol.* doi:10.1085/jgp.200709759.

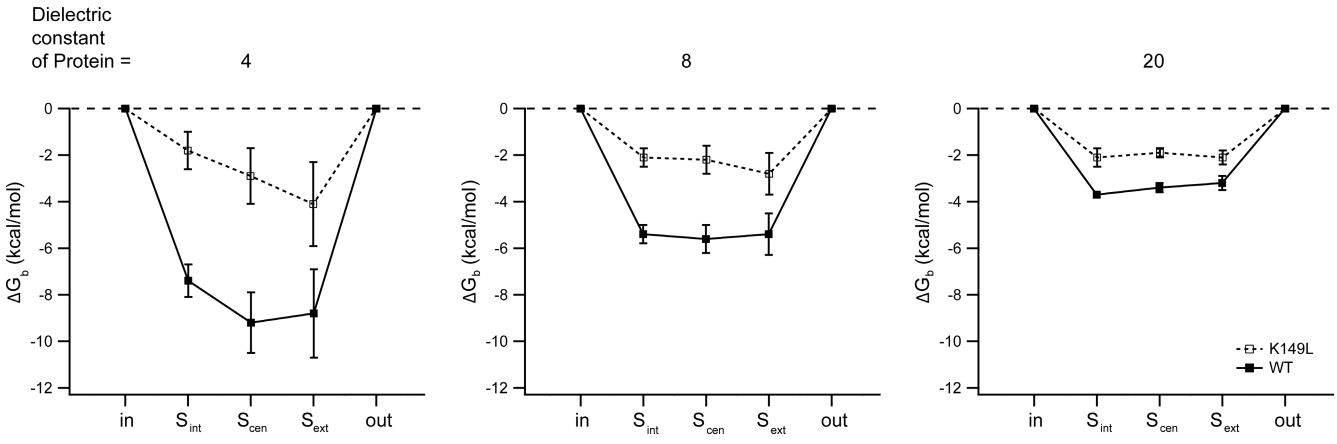

Figure S4. Effect of the dielectric constant on the calculated electrostatic contribution to chloride binding: homology model analysis. As in Fig. 8, we used the wild-type (filled squares) and K149L (open squares) homology models to calculate the electrostatic contribution to the free energy of chloride binding (ΔG_b) to each putative binding site in the pore (starting from the cytoplasmic side: S_{int}, S_{cen}, S_{ext}) when two chlorides are already bound. Reduction in chloride affinity upon substitution of K149 is observed across a wide range of dielectric constant values used, (4, left; 8, middle; and 20, right). Lines connect data points for ease in viewing, and error bars represent an estimate of the discretization error arising from the grid-based Poisson-Boltzmann calculations.

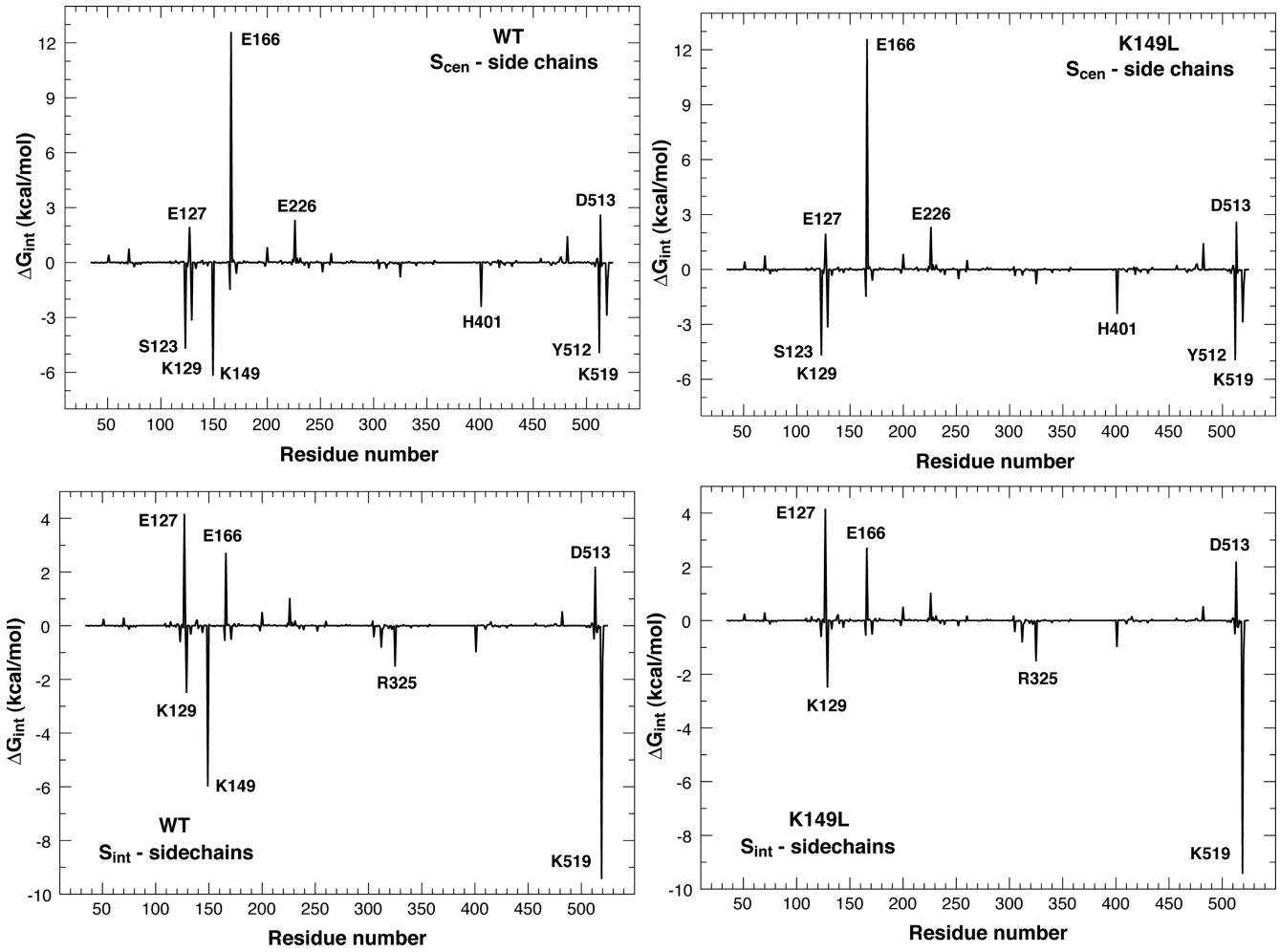

Figure S5. Electrostatic interaction energies between the chloride ion in S_{cen} (top) or S_{int} (bottom) and the side chains of wild-type (left) or K149L (right): homology model analysis. The most prominent interaction peaks are consistent with the known functional importance of the ClC-0 residues, e.g., S123, E166, K149, and K519. Note that the K149L mutation has little effect on the magnitude of the interaction energies between chloride and side chains (other than K149 itself), since the modeling of K149L ClC-0 results in no significant structural changes elsewhere in the protein.

TABLE S1

Gating parameters for four K149 mutants

		$[Cl]_{ext}$ (mM)						
gating parameter	149 side-chain	5	15	30	65	110	310	610
V_o (mV)	M	−3	−17	−32	−46	−61	−82	−87
	R	2	−19	−33	−49	−56	−77	−83
	S	11	9	−8	−21	−35	−55	−52
	L	39	16	6	−11	−25	−41	−45
z	M	0.66	0.66	0.67	0.63	0.63	0.60	0.53
	R	0.65	0.68	0.70	0.72	0.66	0.68	0.68
	S	0.74	0.78	0.80	0.81	0.73	0.77	0.66
	L	0.74	0.78	0.74	0.79	0.78	0.62	0.61
P_{min}	M	0.01	0.00	0.01	0.00	0.01	0.00	0.00
	R	0.01	0.00	0.01	0.01	0.00	0.00	0.09
	S	0.02	0.02	0.03	0.02	0.01	0.01	−0.02
	L	0.01	0.01	0.00	0.01	0.01	0.00	0.00

Plots of apparent open probability (P_o) versus voltage (Fig. 3, B–E) were fit as described in Materials and methods to derive the voltage at the midpoint in the voltage–activation curve (V_o), apparent gating charge (z), and minimum open probability (P_{min}).

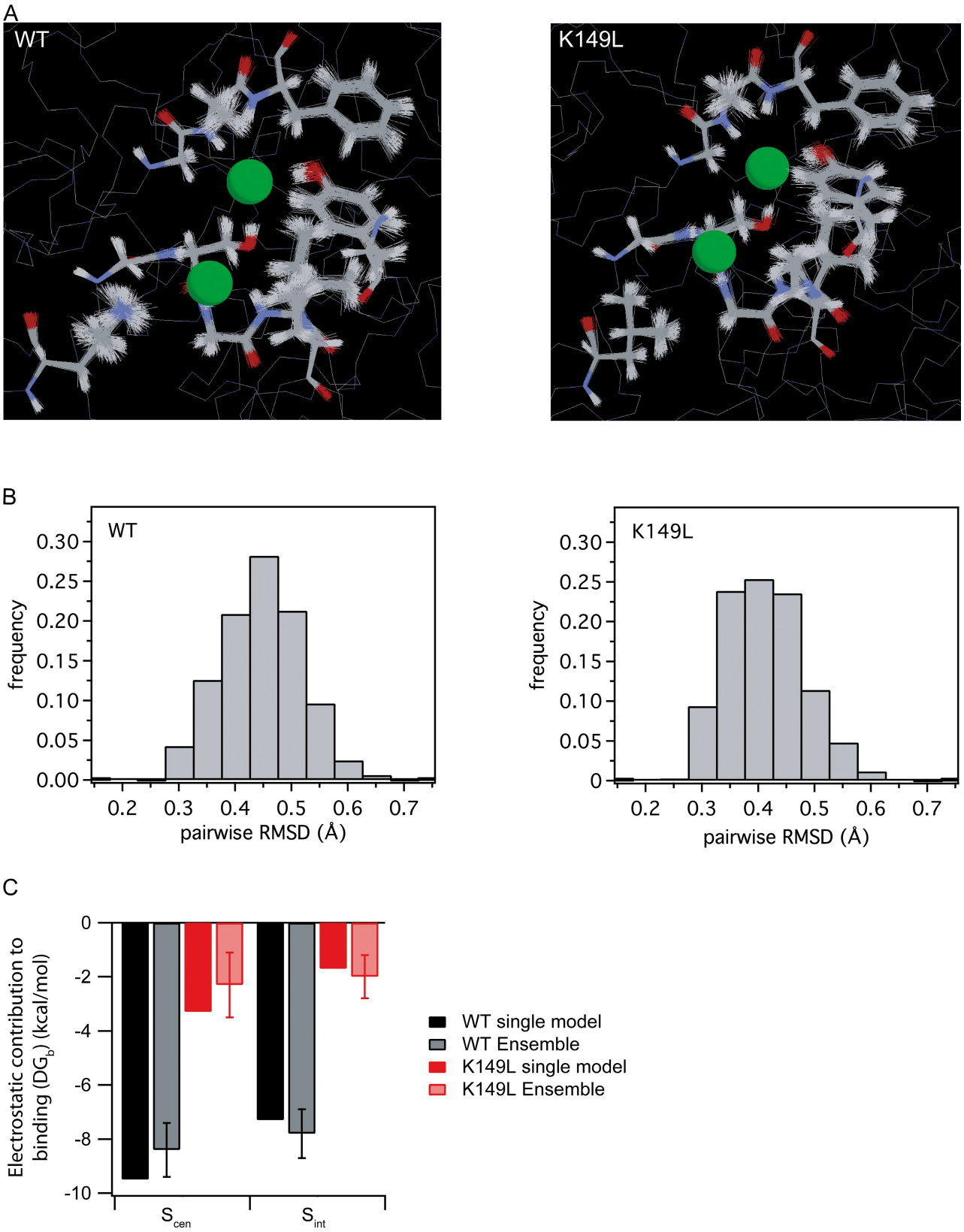

Figure S6. Assessment of the effect of small variations in the structural model on the electrostatics calculations. (A) Molecular graphics overlay of the 100 conformations derived for the wild-type homology model (left) and the K149 homology model (right). (B) Histogram showing the distribution of pairwise RMSD between the conformations in A. (C) Calculated electrostatic contribution to chloride binding for the single models (same data as shown in Fig. 8 in the main text) and for each ensemble of conformations.